L. J. Hart-Smith[1]

Designing to Minimize Peel Stresses in Adhesive-Bonded Joints

REFERENCE: Hart-Smith, L. J., **"Designing to Minimize Peel Stresses in Adhesive-Bonded Joints,"** *Delamination and Debonding of Materials, ASTM STP 876*, W. S. Johnson, Ed., American Society for Testing and Materials, Philadelphia, 1985, pp. 238–266.

ABSTRACT: The same analyses that show how severe the peel stresses can be in adhesively bonded test coupons indicate that those stresses can be reduced to insignificance in structurally configured joints. The successful design of adhesively bonded joints is shown to require the use of adequately long and thin overlaps to ensure that the development of parasitic peel stresses is suppressed, allowing the joint to develop the full shear strength of the adhesives or, better yet, the full strength of the adherends outside the bonded joint. The joint configurations discussed include single-lap joints, single-strap joints, double-lap joints, and skin-to-stiffener joints. The material presented includes both parametric solutions and specific joint analyses to quantify the issues.

KEY WORDS: adhesive bonding, adhesive joints, peel stresses, single-lap joints, single-strap joints, stress analysis, structural design, adhesive test coupons

Nomenclature

- c Half the length of the bonded overlap in the direction of the applied load, m
- D Bending stiffness of the adherends, per unit width, N·m
- E Young's modulus of the adherends, N/m^2
- E_c Transverse modulus of adhesive (cement) in peel, N/m^2
- E_c' Effective peel modulus of adhesive, allowing also for flexibility of resin in laminates, N/m^2
- F_{ty} Yield strength of adherends under tensile loads, N/m^2

[1]Douglas Aircraft Co., McDonnell Douglas Corp., Long Beach, CA 90846.

k	Eccentricity factor for bending of adherends in single-lap or single-strap joints
k_t	Stress concentration factor for adherends under combined stretching and bending loads
ℓ	Length of bonded overlap in direction of applied load, m
M	Bending moment in adherend, per unit width, N
M_e	Adherend bending moment at end of overlap, per unit width, N
M_m	Adherend bending moment in middle of splice plate, per unit width, N
P	Applied load, per unit width, N/m
t	Thickness of adherend, m
t_d	Thickness of doubler, m
t_s	Thickness of skin, m
η	Adhesive layer thickness, m
η	Joint efficiency
ν	Poisson's ratio of adherends
ξ	Exponent, m^{-1}
σ	Stress, N/m^2
σ_{avg}, σ_b, σ_{max}, σ_{remote}	Adherend stresses, N/m^2
σ_c, σ_{peel}	Adhesive transverse tensile stresses, N/m^2
τ, τ_p	Adhesive shear stresses, N/m^2

Introduction

The subject of peel stresses in adhesively bonded joints and advanced fibrous composite structures has gained prominence during the past few years. Special test coupons have been developed for characterizing this behavior in each of the basic modes—tension, shear, and twisting. Much data have been accumulated on the related subject of the growth of flaws in bonded joints or delaminations in composites. Further, information has been developed in the context of the disbond area versus number of cycles (da/dN), along the lines of the requirements of MIL-83444 for the growth of through-cracks in metallic structures.

These investigations have led to the realization that the commercially manufactured toughened adhesives provide a level of toughness and resistance to crack propagation that is so great as to render the application of the basic theory of fracture mechanics questionable. The parallel case in metals is the toughness of wide sheets of 2024 aluminum alloy—it is so tough that classical fracture mechanics analysis is almost unnecessary. On the other hand, the need for damage tolerance analysis for such brittle metal alloys as D6AC and H-11 steels, and 7075-T6 (otherwise known as underaged 7075-T73) and 7079-T6 aluminum alloys, is well established. An equivalent situation has

arisen in the investigation of the fracture mechanics of adhesives and resins. The validity of the theory has been demonstrated on brittle, unmodified polymers which are so lacking in toughness as to create the impression that this subject is of vital importance to the safe application of all bonded or composite structures. Such a conclusion, of course, ignores the reality of 40 years of successful service of Redux-bonded metal structures from deHavilland and from Fokker that were designed before fracture mechanics analysis was applied to any part of the aircraft structure.

Similarly, there has been no concern about fiberglass-epoxy composites that have been cured at temperatures ranging between 120°C (250°F) and room temperature. What damage has been sustained by such laminates has become easily visible, frequently with broken fibers on the surface to warn of the need for repair. Also, there has been little tendency for delaminations in such composites to propagate because the resins cured at low temperatures are much tougher than those cured at 180°C (350°F). Also, the lower cure temperatures do not result in a stressed matrix full of microcracks. While some of these composites have been used for lightly loaded secondary structures such as fairings, others have been used for the entire wing structure on sailplanes and general aviation aircraft.

However, the desire to apply primary composite or metal bonded structures in conditions where the service temperatures range from −54°C (−65°F) to more than 93°C (200°F) has led to the elimination of the usual toughening or plasticizing additives. That has resulted in materials for which fracture mechanics is applicable and, to some extent, necessary because those materials are prone to failure by instantaneous spreading of delaminations under the action of peel stresses around the periphery of the delamination.

Even so, the case for government regulations of the MIL-83444 type being applied to fibrous composites or adhesive bonds is tenuous, at best. The modes of failure of those materials and of metal alloys differ tremendously, as explained in Ref *1*. More importantly, well-designed adhesively bonded joints are always stronger than the surrounding structure. Only if the adhesive were the critical element in the load path would calculations of the estimated service life of adhesive bonds be necessary and, then, all the benefits of adhesive bonding would be lost. In such a case, there shoud be even more concern about static strength than fatigue life. An adhesively bonded joint that has been designed too weak or has a global deficiency because of improper surface preparation could unzip catastrophically over the entire bond area if the surrounding structure were strong enough to overload the adhesive. Also, test data pertaining to this subject are often generated on specimens that bear no resemblance to real structural configurations. Consequently, when the real structures are tested, the failures always occur somewhere else.

This problem is far from unique; the most useful design data for adhesively bonded joints are generated on the thick-adherend short-overlap specimen [*2*] used in conjunction with the KGR-I extensometer [*3*]. However, no one

would seriously consider adhesively bonding 9 to 13 mm (3/8 or 1/2 in.) aluminum alloy plate together with a single-lap joint, as a structural joint, because the adhesive bond would obviously be too weak in comparison with the adherends.

There is a need to place in proper perspective individual articles on the subject of peel stresses and fracture mechanics in adhesive bonds and fibrous composite structures. This paper explains the gross differences between peel stresses in test coupons that are proportioned to force a failure in a particular mode, and peel stresses in structurally configured joints where the object is usually to eliminate that particular mode in order to maximize the joint strength. With that knowledge, the designer is able to avoid bonded joint configurations that suffer from weaknesses associated with high peel stresses in the adhesive.

This paper draws heavily upon the analyses in Ref *4*, from which the equations given here have been quoted.

Single-Lap Joints Between Identical Adherends

The existence of substantial induced peel stresses at the ends of the overlaps of single-lap adhesively bonded joints has been known for 40 years since the classical analysis by Goland and Reissner in Ref *5*. Detailed analyses have shown repeatedly that the failure of such a coupon is rarely if ever affected by the shear strength of most adhesives. Consequently, the adoption of the standard ASTM Test Method for Strength Properties of Adhesives in Shear by Tension Loading (Metal-to-Metal) (D 1002) test coupon, shown in Fig. 1, as the almost universal standard test for the shear strength of adhesive has baffled many investigators (see, for example, Ref *6*). Nevertheless, it should be acknowledged as an effective and inexpensive quality assurance coupon, when used in conjunction with cure-monitoring records and with tests to verify the adequacy of the preparation of the surfaces for bonding.

The deformation under load of this coupon, in particular, and of single-lap joints, in general, is described in Fig. 2. Were the applied load to be compressive instead of tensile, the bonded overlap would rotate in the opposite direction to that shown and the specimen would need to be stabilized against buckling. Unsupported single-lap joints are therefore used only to transfer tensile or in-plane shear loads. In the latter case, there would be no peel stresses

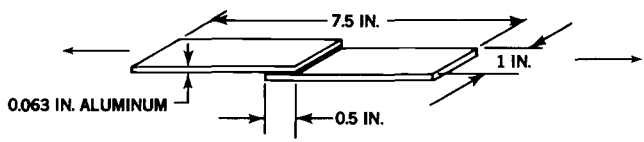

FIG. 1—*Standard lap shear bond test (1 in. = 25.4 mm).*

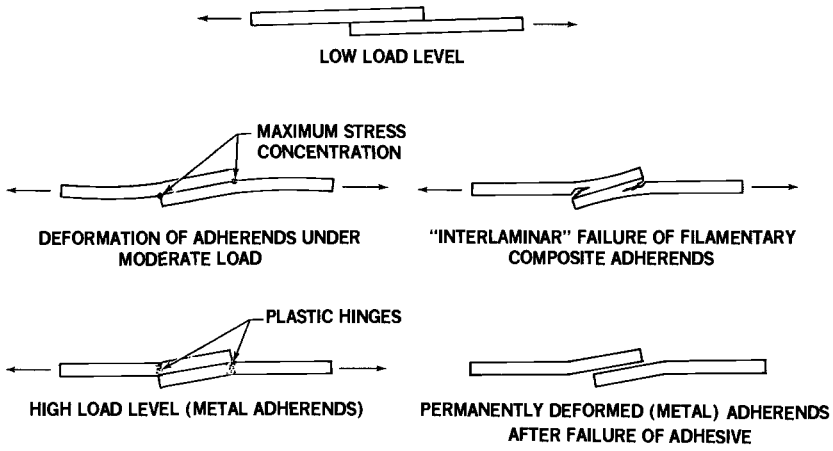

FIG. 2—*Single-lap bonded joints with eccentric load path (brittle and ductile adherends).*

around most of the periphery of the bonded area because there would be no out-of-plane deformations. Any peel stresses would then be confined to four small areas in the extreme corners of the bond.

In the usual case of application of tensile lap shear loads, the peak adhesive peel stress at the ends of the overlaps is

$$\sigma_{c\max} = M_e \sqrt{\frac{E_c}{2\eta D}} \tag{1}$$

where

E_c = transverse peel modulus of the adhesive,
η = thickness of the adhesive layer,
D = bending stiffness of the adherends, and
M_e = bending moment in the adherends at the ends of the overlap.

That bending moment, in turn, is given by

$$M_e = \frac{P\,(t + \eta)/2}{\left[1 + \xi c + \frac{1}{6}\xi^2 c^2\right]} = \mathrm{kP}\,(t + \eta)/2 \tag{2}$$

where

t = adherend thickness,
P = applied tensile load per unit width, and
c = half the bonded overlap in the direction of the applied load.

The exponent ξ is given by

$$\xi = \sqrt{P/D} \tag{3}$$

The peak peel stress is thus proportional to the adherend bending moment M_e, which decreases as the overlap increases in the manner described in Fig. 3. The figure also shows that Goland and Reissner overestimated that bending moment by making unnecessary approximations. If the standard lap-shear specimen were characterized thoroughly on the basis of their analysis, the peel stresses would appear to be even more dominant than they actually are. That makes the acceptance of the ASTM D 1002 specimen for shear testing of adhesives even more difficult to comprehend.

It should be noted in all the equations given here, and those derived in Ref *4*, that the thickness η of the adhesive layer is everywhere taken to be negligibly small (but not zero) in comparison with the thickness t of the adherends. The adherend bending moments M would be increased by the added eccentricity in load path in any case in which that simplification could not be justified.

Figures 4 and 5 characterize the failure modes and strengths of single-lap bonded joints between aluminum alloy adherends as a ratio of the joint strength to the adherend strength remote from the joint. There are three distinct failure modes, each of which has been analyzed independently of the others. The modes are: adherend failure under combined stretching and bending, adhesive shear, and adhesive peel. Normally, one mode will dominate over the others; for a small regime at the intersection between modes, the separate analyses will overestimate the actual strength and the transition will

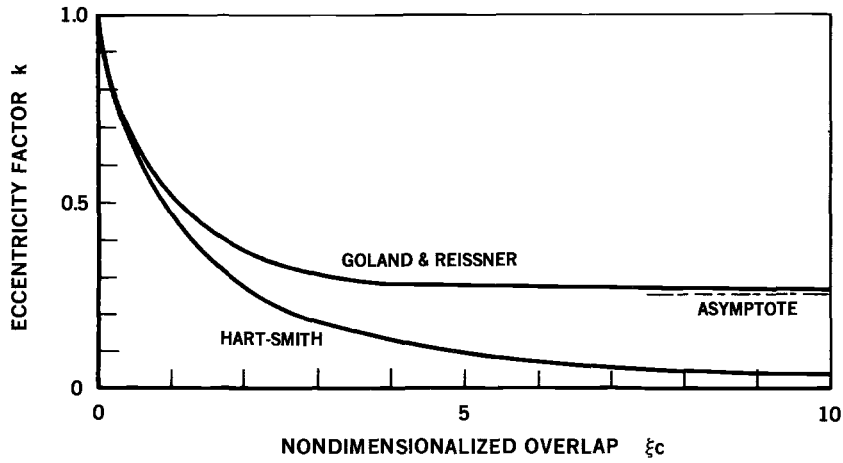

FIG. 3—*Comparison between solutions for adherend bending stresses in single-lap bonded joints.*

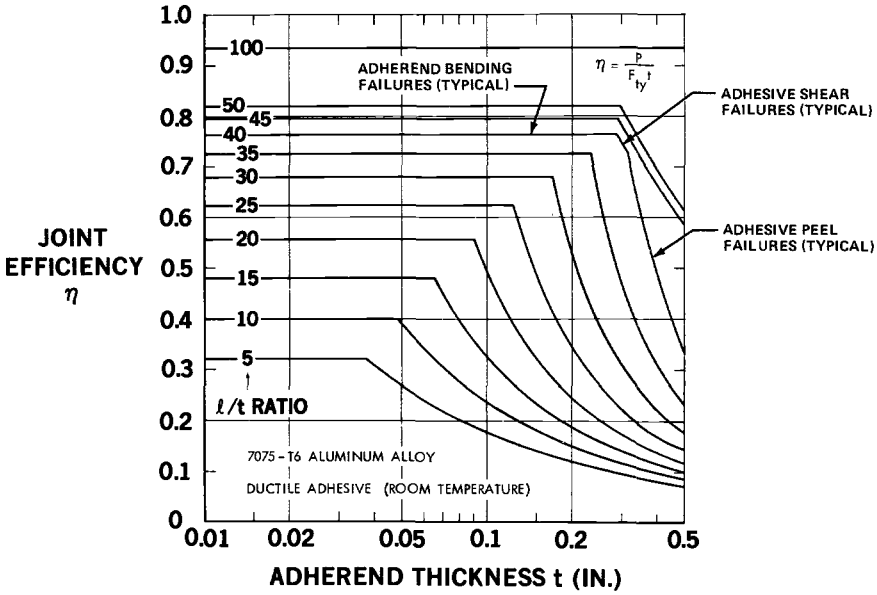

FIG. 4—*Joint efficiency chart for single-lap bonded joints (ductile adhesive) (1 in. = 25.4 mm).*

occur gradually rather than abruptly, as shown. The horizontal lines refer to failure of the adherends at the ends of the overlap, from a combination of direct stretching and bending loads. Note how much stronger the joints are for the longer overlaps; at an overlap-to-thickness ratio (ℓ/t) of 8, as used on test coupons, the structural efficiency is barely 36%, while for an ℓ/t of 80 that is more typical of structural joints the efficiency is raised to better than 90%. The small weight penalty in the vicinity of the longer splice is insignificant in comparison with the weight saving in the entire basic skin.

The mechanism behind the dramatic sensitivity to the ℓ/t ratio is explained by the relation

$$\eta = \frac{\sigma_{avg}}{\sigma_{max}} = \frac{P/t}{P/t + 6M/t^2} = \frac{1}{1 + 3k} \tag{4}$$

where k is the alleviation factor defined by Eq 2. This relationship is depicted in Fig. 6. Figures 4 and 5 show that, for aluminum adherends less than 1.2 mm (0.05 in.) thick, this adherend bending is the dominant failure mode for all ℓ/t ratios. Here, $\ell = 2c$ is the total bonded overlap. The dominant failure mode for thicker adherends is shown by the same two figures to be by peel, as expressed by Eq 1 and 2. There are only very small areas of shear dominated failures of the adhesive; for $\ell/t > 35$ in conjunction with $t > 6$ mm (0.25 in.) for the ductile adhesive and for $\ell/t > 25$, with $t > 3$ mm (0.13 in.) for brittle

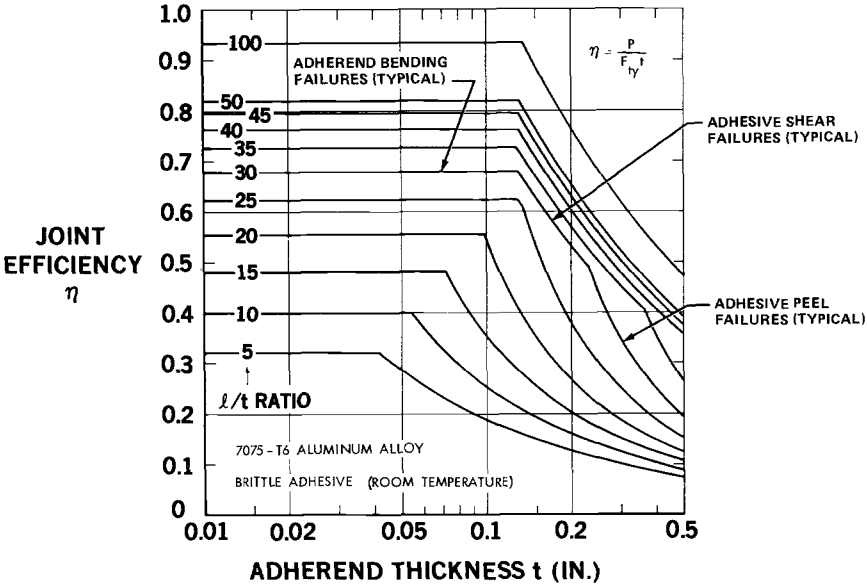

FIG. 5—*Joint efficiency chart for single-lap bonded joints (brittle adhesive) (1 in. = 25.4 mm).*

(high service temperature) adhesives. The analysis of the associated adhesive shear stresses is presented in Ref *7*.

Figures 4 and 5 reveal that, for each adherend thickness, a simple change in overlap can effect a dramatic change in failure mode. The adhesive peel stresses that so dominate the behavior of short-overlap test coupons can be reduced to insignificance in structural joints by the use of an adequate overlap. Consequently, the characterization of behavior measured on such a test coupon would be irrelevant to properly proportioned structural joints. This is confirmed by fatigue tests on long-overlap joints that fail consistently not in the adhesive at all, but in the adherends immediately outside the bonded overlap (see Ref *8*, for example).

Much the same phenomenon arose in the accelerated versus real-time testing of adhesively bonded joints during the Primary Adhesively Bonded Structure Technology (PABST) program [*8*]. Accelerated testing of coupons gave misleading results in the sense that apparent weaknesses were exposed by the elimination of the creep resistance inherent in long-overlap joints or were hidden by cyclic load applications so frequent that the load was being removed again before the adhesive in the test coupons had a chance to creep. Once the actual mechanisms acting on the adhesive had been identified, it took a four-year-long test program of near-to-real-time testing of structurally configured joints in a hostile hot/wet environment to prove that there was no need for concern about the long-term durability of adhesively bonded structures. The work in Ref *8* has been followed by fundamental research, in Ref *9* for exam-

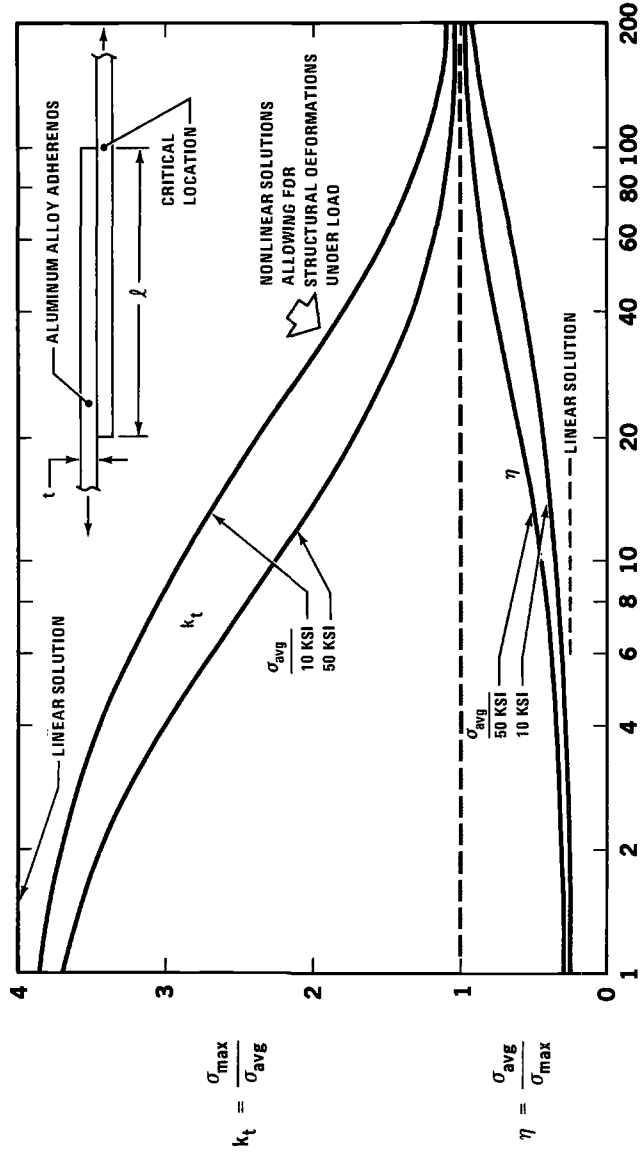

FIG. 6—*Adherend stress concentration and joint efficiency of single-lap joints (1 ksi = 6.9 MPa).*

ple, into the subject characterizing accelerated testing of adhesives and relating those results to behavior in service. Results to date indicate that the time-dependency of the behavior of adhesives greatly complicates this subject.

Even in those areas of Figs. 4 and 5 where peel stresses are predicted to be dominant, these stresses can be diminished very greatly by locally tapering the ends of the overlap to be no more than 0.8 mm (0.03 in.) thick. The ratio of the adhesive peel stresses with and without tapering is

$$\frac{(\sigma_{c_{max}})_{\text{tapered}}}{(\sigma_{c_{max}})_{\text{uniform}}} = \sqrt{\frac{2}{1 + \left(\frac{t}{t_e}\right)^3}} \tag{5}$$

where t_e is the reduced thickness of the adherend at the ends of the overlap. A twofold reduction in adherend tip thickness corresponds to adhesive peel stresses that are reduced to only 47% as severe as without such tapering. Again, a very simple design modification is shown to be capable of diminishing the effect of the peel stresses below that which an assessment of simple test coupons would have suggested.

Indeed, the combination of an adequate overlap with sufficiently thin ends of the adherends is enough to eliminate all effects of adhesive peel stresses on single-lap joints (Fig. 7). The peak peel stress in the structurally configured joint shown in only 3.5% as high as in the equivalent ASTM D 1002 test coupon shown. Then, with thin adherends that are typically less than 2 mm (0.08 in.) thick, such bonded joints fail outside the overlap or, for thicker adherends, they fail in the adhesive by shear. Under such circumstances, the analysis of adhesive peel stresses is not made to characterize the strength or life of such joints, but to identify those joint geometries which need modification so that the peel stresses can be reduced to insignificance.

Single-Lap Joints Between Dissimilar Adherends

The induced peel stresses are equally severe at both ends of a single-lap bonded joint when the adherends are identical. However, when one adherend is thicker than the other, both the adherend bending moment and the peak adhesive peel stress are intensified at the end of the joint from which the thinner adherend extends. The relevant analyses are given in Ref 7. Figure 8 shows how this stiffness imbalance reduces the adherend bending strength of such a joint. Figure 9 presents the associated increases in the adhesive peel stresses for one particular value of the nondimensionalized peel stress coefficient, C_{PEEL}. The obvious response of the aircraft designer to such information is to avoid the use of such unbalanced joints, rather than to accept the deficiencies inherent in them. Again, the merit of the analysis of adhesive peel stresses in such joints is to identify geometries which should not be used, rather than to provide data relevant to design of useful structure.

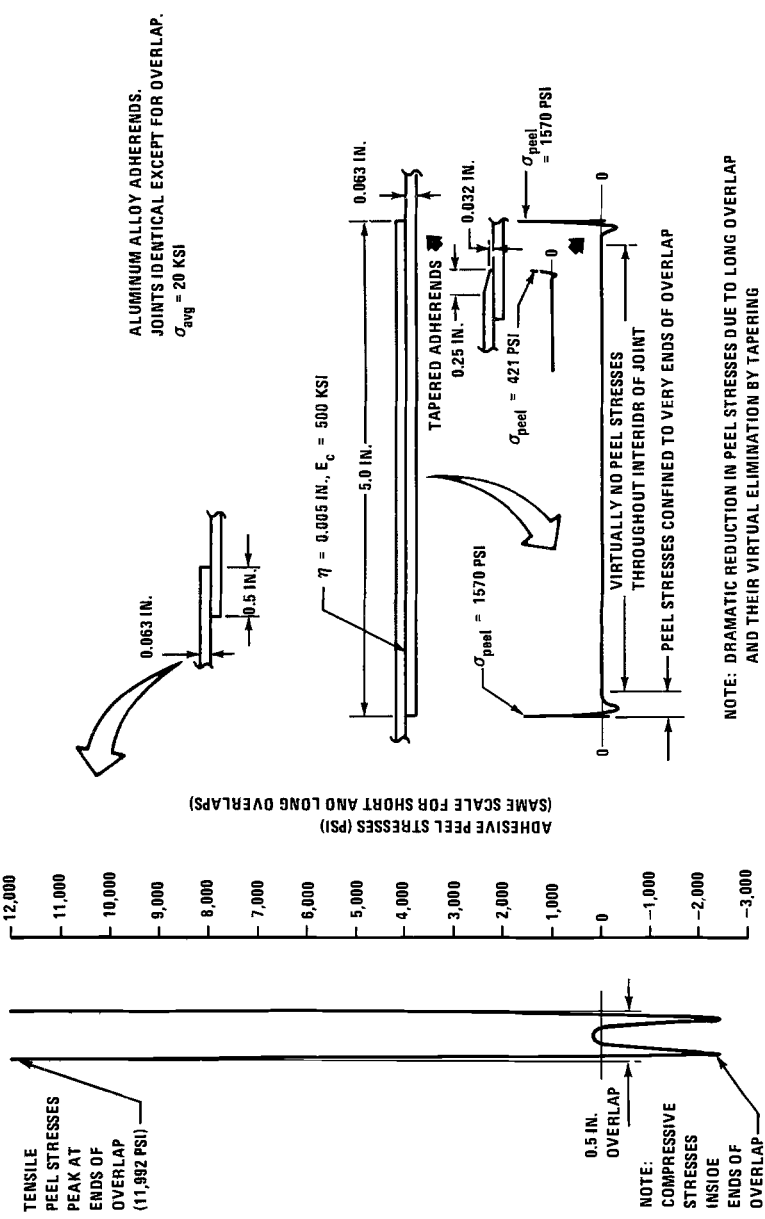

FIG. 7—*Adhesive peel stresses in short- and long-overlap single-lap bonded joints (1 in. = 25.4 mm; 1 ksi = 6.9 MPa; 1 psi = 6.9 kPa).*

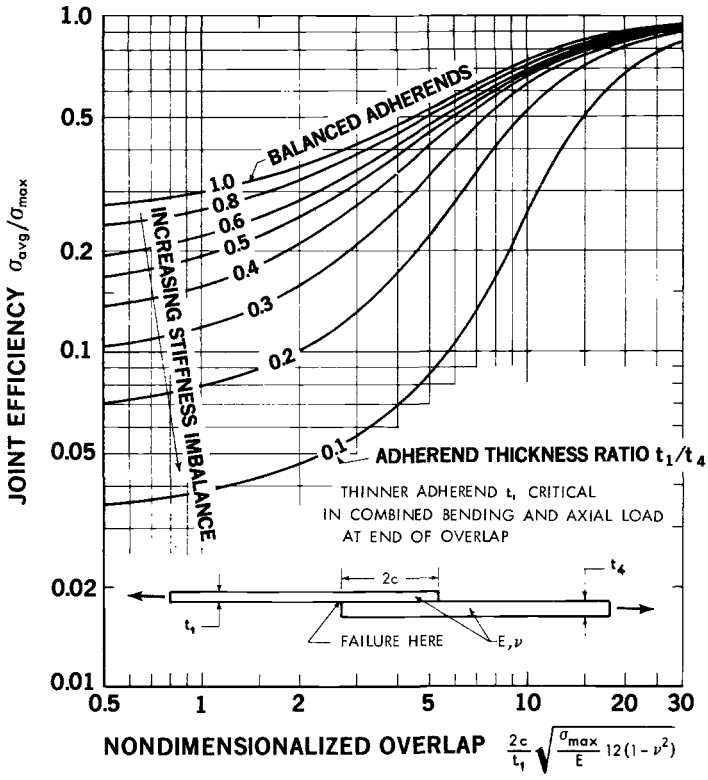

FIG. 8—*Effect of adherend stiffness imbalance on adherend bending strength of single-lap bonded joints.*

Single-Strap Bonded Joints

The use of a long bonded overlap was shown above to improve substantially the strength of single-lap adhesively bonded joints because the eccentricity in overlap could then be alleviated by gentle out-of-place deflections. In the case of a flush bonded joint (Fig. 10) there must inevitably be an abrupt discontinuity precisely where the skins butt together. Consequently, the single-strap or flush bonded joint has more severe induced peel stresses in the adhesive than any other kind of skin splice. Indeed, such a joint barely qualifies as a means of transferring load; a better description would be as a built-in stress concentration. This was the only form of bonded joint to exhibit any flaw growth in the series of tests reported in Ref *10*.

The bending moments in the adherends at the middle and ends of the splice differ for the single-strap joint. The respective values are

$$\frac{M_m}{P\left(\frac{t_s + t_d}{2} + \eta\right)} = \frac{1}{\left[1 + \frac{\left(1 + \frac{2}{3}\xi_s c + \frac{1}{12}\xi_s^2 c^2\right)}{\left(\frac{t_d}{t_s}\right)^3 \left(1 + \frac{4}{\xi_s c}\right)}\right]} \tag{6}$$

and

$$\frac{M_e}{P\left(\frac{t_s + t_d}{2} + \eta\right)} = \frac{1}{\left[1 + \frac{2}{3}\xi_s c + \frac{1}{12}\xi_s^2 c^2 + \left(\frac{t_d}{t_s}\right)^3 \left(1 + \frac{4}{\xi_s c}\right)\right]} \tag{7}$$

The quantities involved in these equations are the same as in Eqs 1 to 3 except that here c refers to the full value of each overlap, ℓ. These expressions are

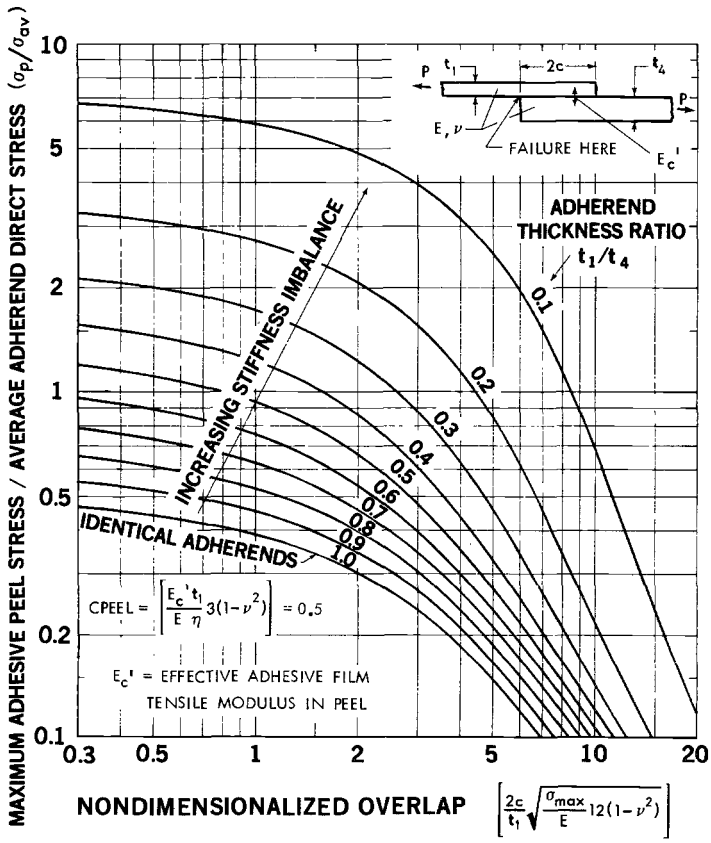

FIG. 9—*Effect of adherend stiffness imbalance on peel stresses in single-lap bonded joints.*

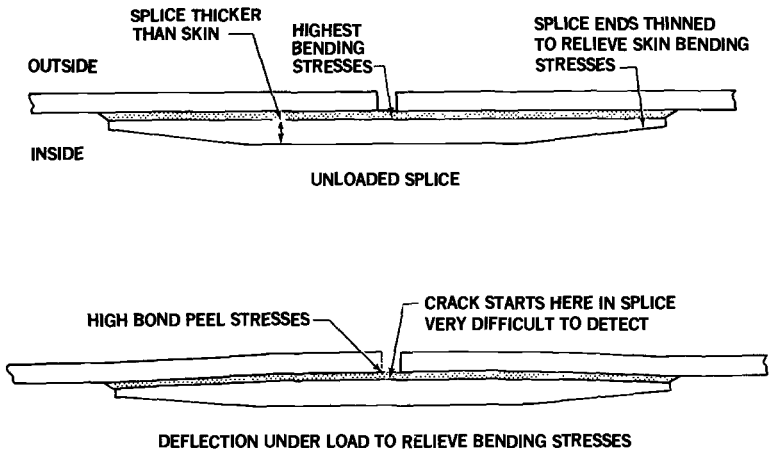

FIG. 10—*Single-strap (flush) splices.*

depicted nondimensionally in Fig. 11. Again, it is evident that a sufficiently long overlap is capable of restricting the magnitude of both bending moments. Likewise, a short overlap would be associated with severe bending moments in both adherends.

The more severe bending moment in the splice plate suggests the use of a splice plate thicker than the skin, even though that would aggravate the basic eccentricity in load path. Typical adherend bending moments in such a case are shown in Fig. 12, but that does not really demonstrate whether the net effect on the peak adherend stress is beneficial or detrimental.

That ambiguity is resolved in Fig. 13, which depicts the ratio of the peak stress in the splice plate to the remote stress in the skin. That ratio is

$$\frac{\sigma_{\max}}{\sigma_{\text{remote}}} = \left(\frac{t_s}{t_d}\right)\left[1 + \frac{3\left(1 + \frac{t_s}{t_d}\right)}{1 + \frac{\left(1 + \frac{2}{3}\xi_s c + \frac{1}{12}\xi_s^2 c^2\right)}{\left(\frac{t_s}{t_d}\right)^3\left(1 + \frac{4}{\xi_s c}\right)}}\right] \tag{8}$$

The reinforcement of the splice plate is seen to be effective only for relatively low overlap-to-thickness ratios; there is no significant difference for the large ℓ/t ratios that would be used on a real structure.

As in unsupported single-lap joints, the peak adhesive peel stresses induced in single-strap bonded joints are proportional to the bending moments at the respective ends of each overlap. The actual expressions are given in Ref *4* and

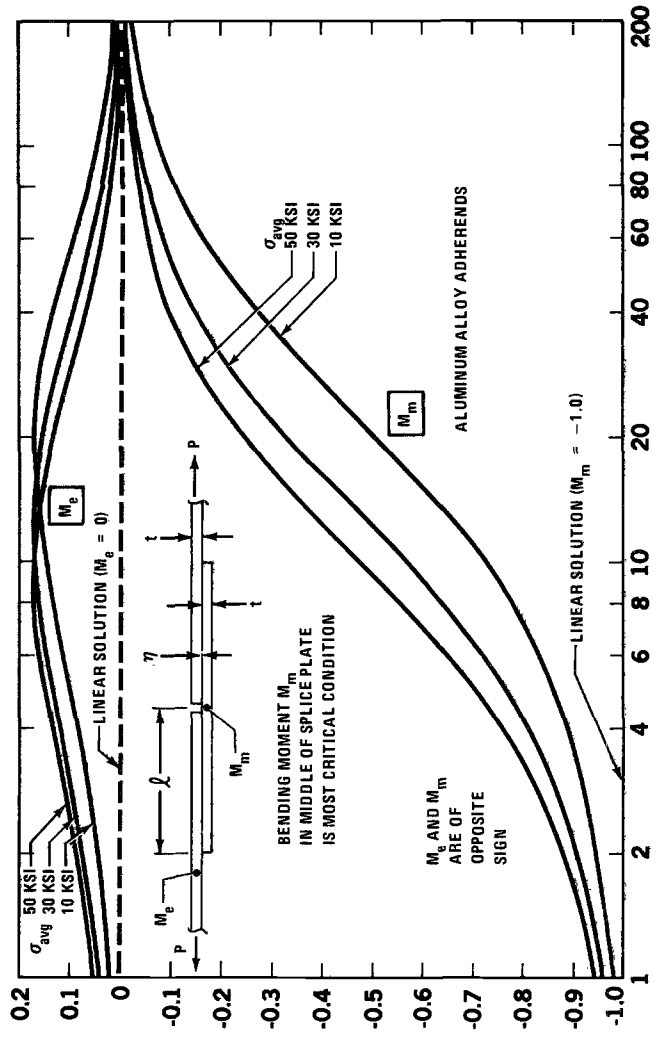

FIG. 11—*Nondimensionalized adherend bending moments in single-strap (flush) joints (1 ksi = 6.9 MPa).*

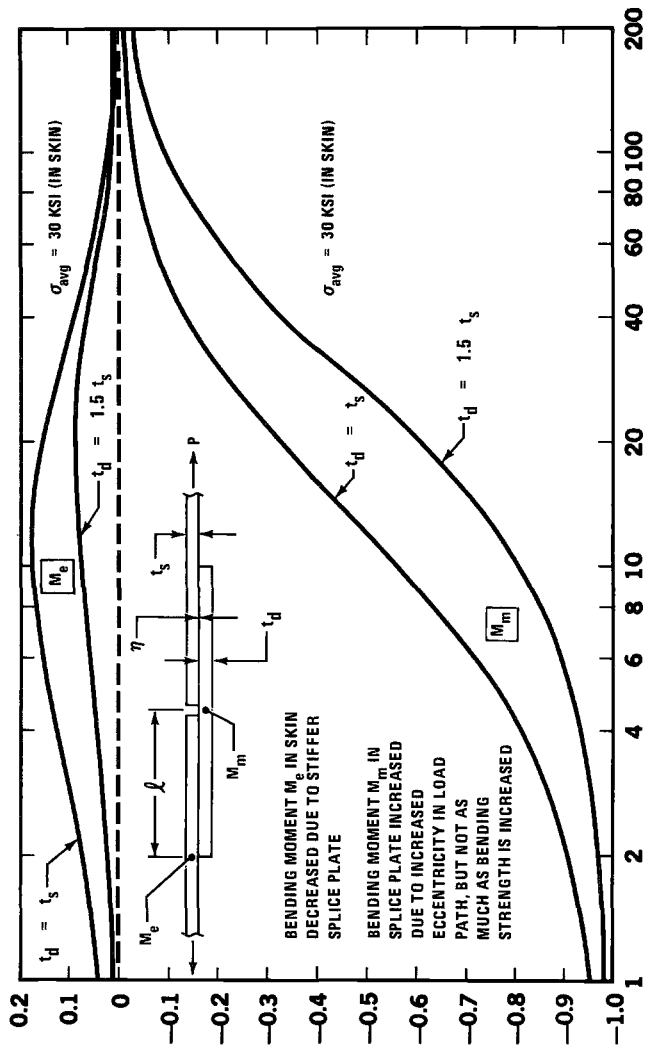

FIG. 12—*Effect of thickened doubler on bending moments in single-strap (flush) joints (1 ksi = 6.9 MPa).*

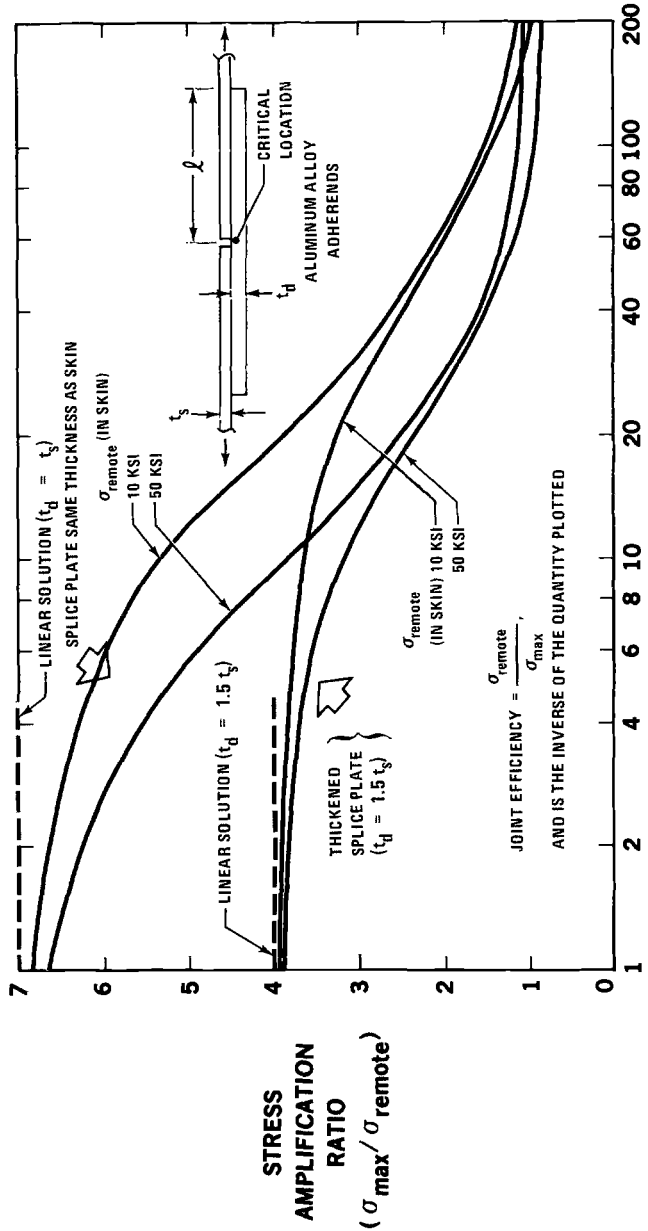

FIG. 13—*Reduction in maximum adherend stress in single-strap joints due to thickened splice plate (1 ksi = 6.9 MPa).*

are omitted here because of their complexity. Figure 14 contains the predicted adhesive peel stresses for a variety of such flush bonded joints. The difference between long and short overlaps reduces the peak induced peel stress by a factor of almost 30 to 1. Actually, the short-overlap joint would have failed long before the remote adherend stress had reached 138 MPa (20 ksi); the adhesive peel stress is limited to about 69 MPa (10 ksi).

Tapering of the skins where they butt together, in conjunction with a local thickening of the adhesive layer, causes a further reduction in the peak adhesive peel stress—to less than 0.15% of the value induced by the same adherend stress in the short-overlap coupon. Fatigue tests on such tapered flush joints are described in Ref *4*. The test program was unfortunately terminated prematurely because of fiscal constraints, but not before comparative testing had confirmed at least a substantial increase in fatigue life resulting from this seemingly minor design refinement.

Not even this joint, with the most severe induced adhesive peel stresses of any bonded joint, must necessarily be handicapped by the possibility of peel-stress failure. The design details needed to suppress such parasitic stresses are simple and practical. Again, the use of adequate overlaps in conjunction with local tapering of the adherends in areas of potentially high peel stresses serves to eliminate such problems.

Improved Flush Bonded Joints

Another technique for dealing with the induced bending moments and peel stresses in single-strap joints is shown in Fig. 15. There is a simultaneous decrease in the eccentricity in load path and an increase in the bending strength and stiffness of the splice plate. The reduction in skin thickness is not a major weakness because roughly half the load in the skin would have already been transferred through the adhesive outside that step.

Figure 16 presents a comparison between the adhesive peel stresses for such a joint with and without this modification. Not only is the peak adhesive peel stress reduced by a factor of four, but the bending stress in the splice plate is also reduced by a factor of nearly two in combination with a one-third reduction in the direct stress. This latter improvement cannot be obtained by the adherend tapering shown in Fig. 14.

A further solution to this design challenge of an efficient flush bonded joint is given in Fig. 17. Here, the approach is to move the notch effect close to a point of inflexion instead of locating it precisely where the bending moment is maximized. The scheme in Fig. 17 also maximizes the splice plate bending strength and stiffness—by a bonded doubler—where the maximum bending moment develops.

The reduction in adhesive bond area with which to transfer the load is not serious because the overlap should be far greater than shear transfer alone would require in order to minimize the bending moments caused by the ec-

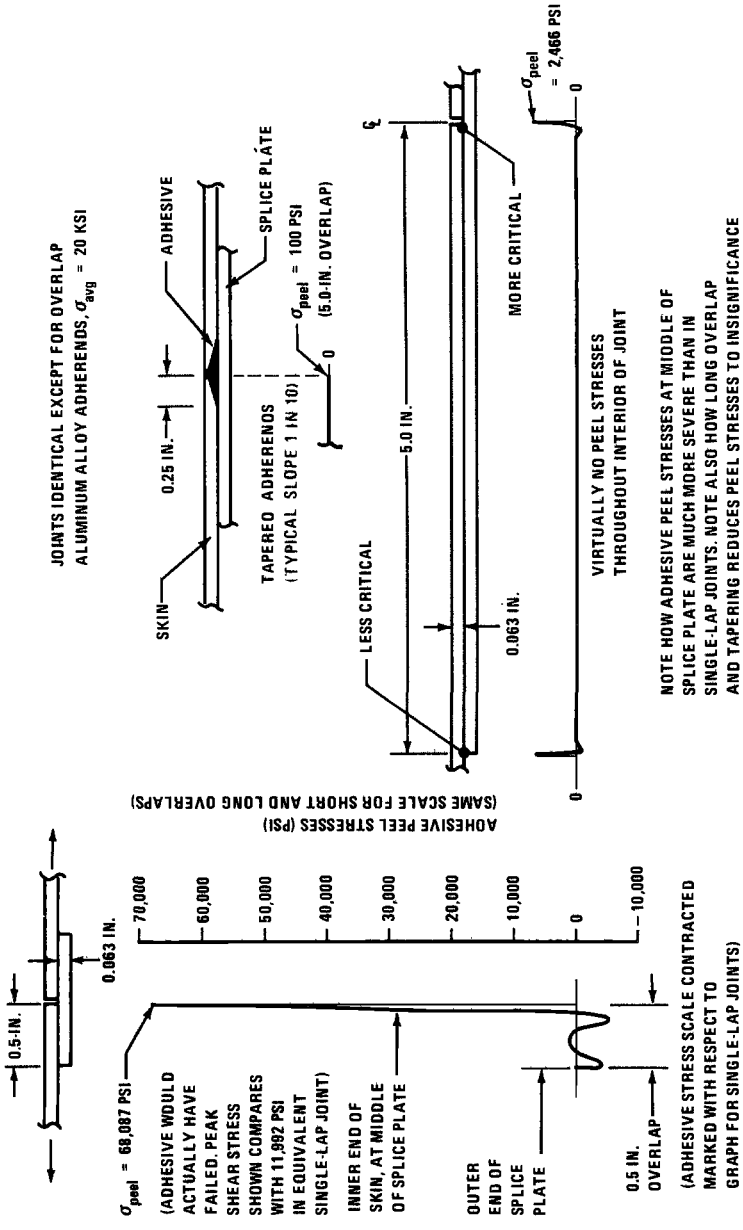

FIG. 14—Adhesive peel stresses in short- and long-overlap single-strap bonded joints (1 in. = 25.4 mm; 1 ksi = 6.9 MPa; 1 psi = 6.9 kPa).

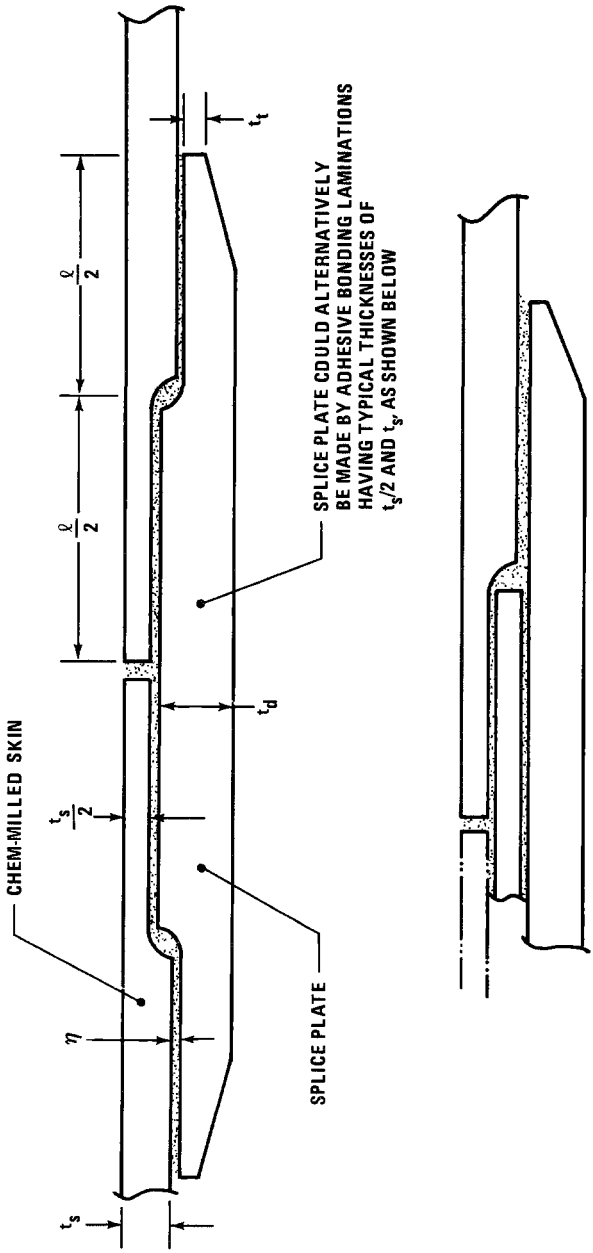

FIG. 15—*Flush bonded joint with reduced eccentricity in load path.*

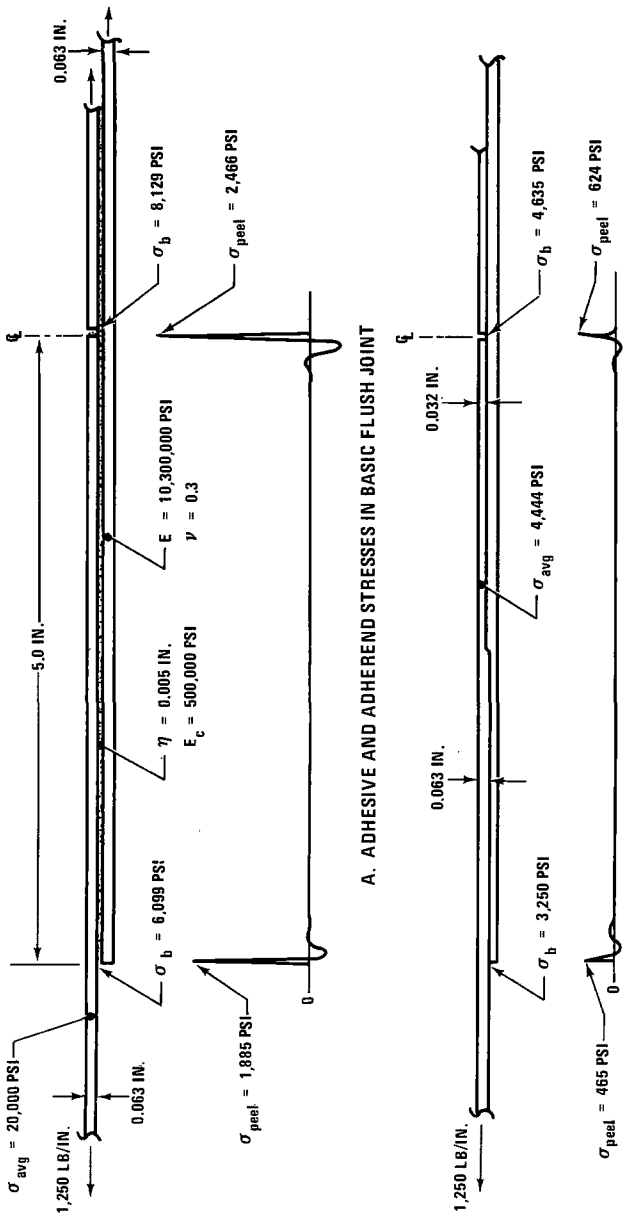

FIG. 16—*Relief of adhesive peel stresses in flush (single-strap) bonded joints (1 in. = 25.4 mm; 1 psi = 6.9 kPa; 1 lb/in. = 0.1129 N·m).*

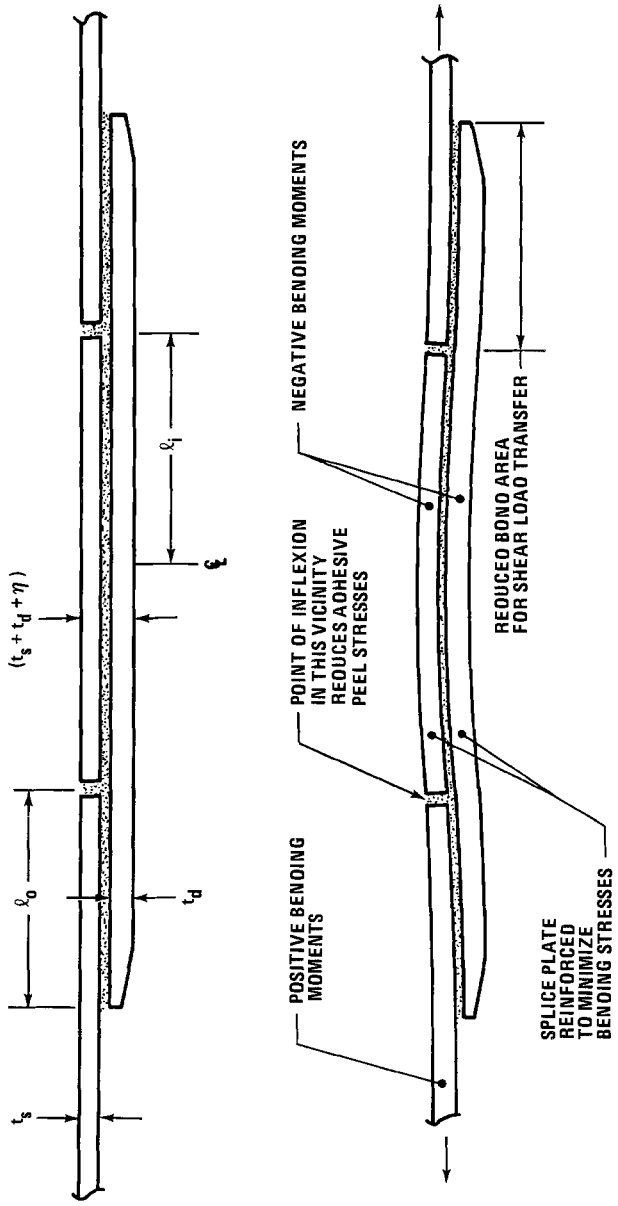

FIG. 17—*Flush bonded joint reinforced at critical location.*

centricity in load path. Figure 18 shows comparative results of the analysis of basic and modified flush bonded joints. The adhesive peel stresses can be virtually eliminated, as shown. The adherend bending stresses are reduced even further than by the modification in Fig. 15.

The analyses of these modified flush bonded joints that are given in Ref *4* and illustrated here confirm again that any induced peel stresses associated with short overlaps can be reduced to insignificance by long overlaps and a little design finesse. Fatigue tests on these improved structural joints would inevitably fail in the adherends, not in the adhesive. The objective of analysis of the adhesive stresses in these joints should not be to predict the life of a weak-link bond, but rather to learn how to maximize the strength and fatigue lives of the adherends. The use of more than a minimum width of splice plate is a small penalty to pay for substantial increases in the structural efficiency of the skins themselves.

Double-Lap or Double-Strap Joints

Despite the lack of any obvious eccentricity in load path of double-lap joints that would be expected to cause the adherends to bend, the splice plates are subjected to bending by the mechanism described in Fig. 19. The peak induced adhesive peel stress is

$$\frac{\sigma_{c_{\max}}}{\tau_p} = \left[\frac{3(1-\nu^2)E_c}{E}\right]^{1/4}\left(\frac{t_0}{\eta}\right)^{1/4} \tag{9}$$

Here, τ_p is the peak adhesive shear stress which is assumed to be constant throughout the small area at the very end of the overlap in which high peel stresses develop. Equation 9 clearly indicates those design modifications that are useful in minimizing the peak adhesive peel stress—a reduction in the tip thickness of the outer adherend and a local increase in the adhesive layer thickness. These details are described in Fig. 20 and were shown to work well during the PABST program. This problem is not subject to the dominant effect of the overlap that is found in joints which contain a basic eccentricity in load path.

The independence of the three possible failure modes of adhesively bonded joints is explained in Fig. 21 in terms of a double-lap joint. The figure shows two possible sequences of failure as a function of adherend thickness, which is the dominant parameter. The adherend strength outside the joint is proportional to its thickness, t, and that strength may be greater or less than the load at which the adhesive could fail. The adhesive would fail according to a $t^{1/2}$ power law for a shear failure [*11*] or a $t^{1/4}$ relation for a peel failure. In other words, the failure mode is a strong function of the adherend thickness (Fig. 21). For sufficiently thin adherends, the weak link will always be in the adher-

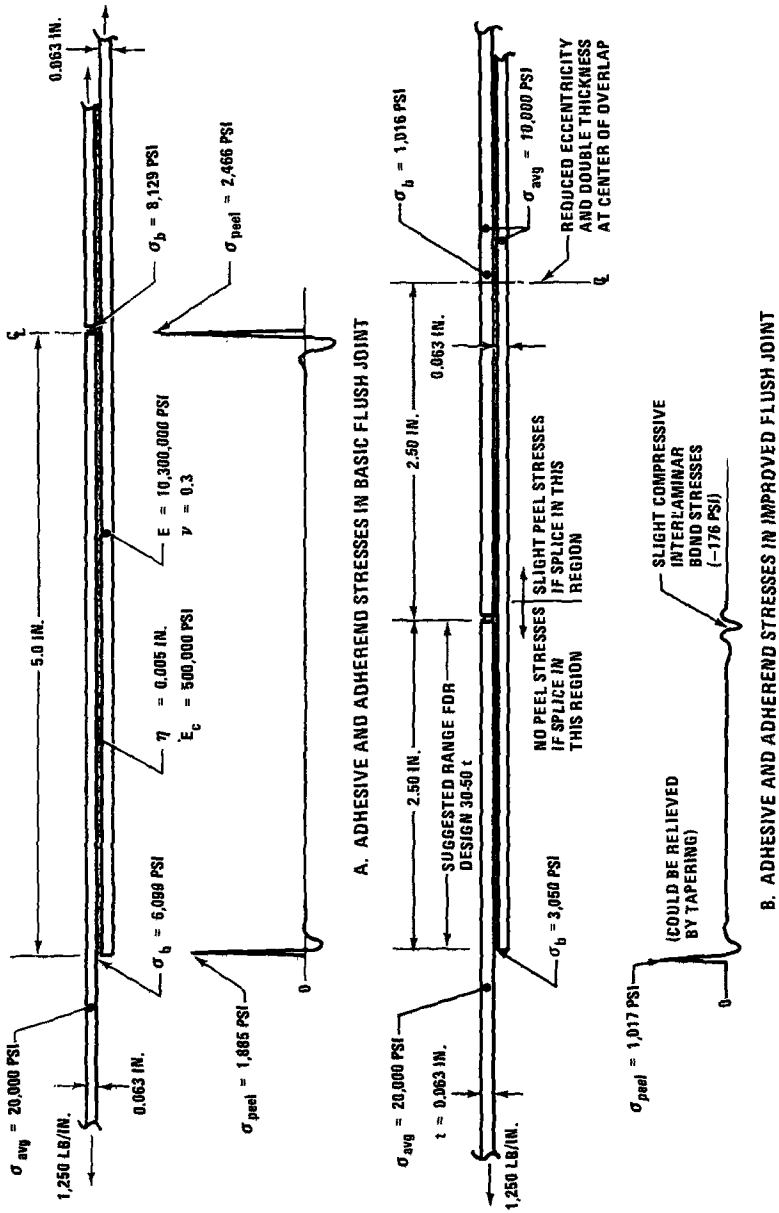

FIG. 18—*Basic and improved designs of single-strap adhesive-bonded joints (1 in. = 25.4 mm; 1 psi = 6.9 kPa; 1 lb/in. = 0.1129 N·m).*

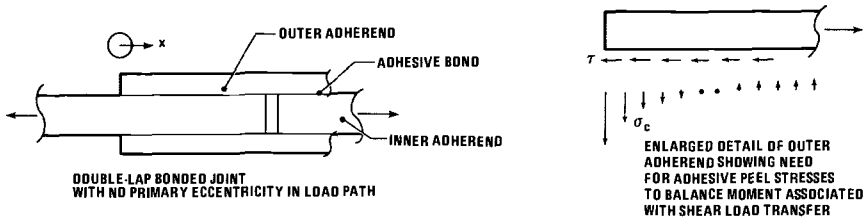

FIG. 19—*Induced peel stresses in double-lap adhesive-bonded joints.*

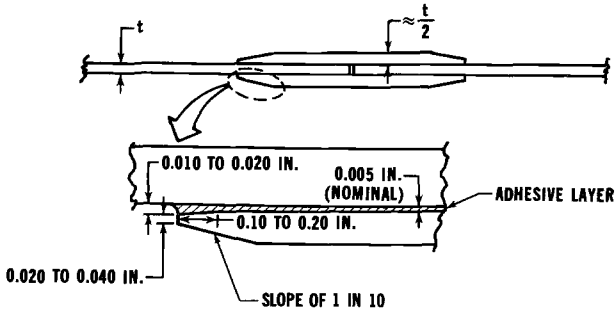

FIG. 20—*Tapering of edges of splice plates to relieve adhesive peel stresses (1 in. = 25.4 mm).*

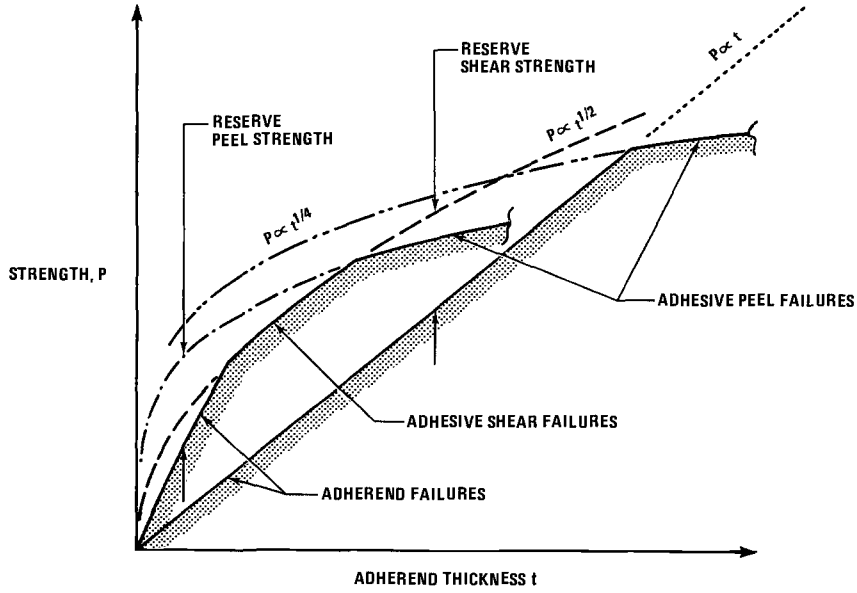

FIG. 21—*Relative severity of adhesive shear and peel stresses.*

ends outside the joint. For slightly thicker adherends, there may or may not be a shear failure. If the adherends are sufficiently thick, the failure will always be by peeling apart the adhesive or composite laminate, unless those curves are raised by some of the modifications discussed here.

It is apparent that the only joint that a test coupon can characterize is the coupon itself. All other joint geometries will have a different mix of adhesive peel and shear stresses.

Tension-Tee Stiffener-to-Skin Bonded Joints

Those bonded joints discussed above have adhesive peel stresses that are induced by the application of a basically shear load. There are also some joints in which the peel stresses are applied directly. Such joints occur between the skin of pressurized fuselages and its internal stiffeners—frames and longerons. There is considerable amplification of the peel stresses in such cases (Fig. 22). Indeed, analyses indicate that almost 49% of the bonded area is trying to push the other 51% apart. The adhesive peel stresses have a distribution governed by the classical beam-on-elastic-foundation equations.

The ratio of peak to average peel stresses in Fig. 22 is strongly influenced by the width-to-thickness ratio (b/t) of the stiffener flange. A large ratio is needed to restrict the peak peel stress that develops right under the outer edges of the stiffener flanges. Locally tapered edges on the flanges also reduce those peak peel stresses. The flexible flange on both sides of the stiffener web reduces the peak peel stress far below the stresses that would develop under the abrupt heel of a Z or angle stiffener. The considerations that led to the sizing of the longerons and frame tees for the PABST program are explained

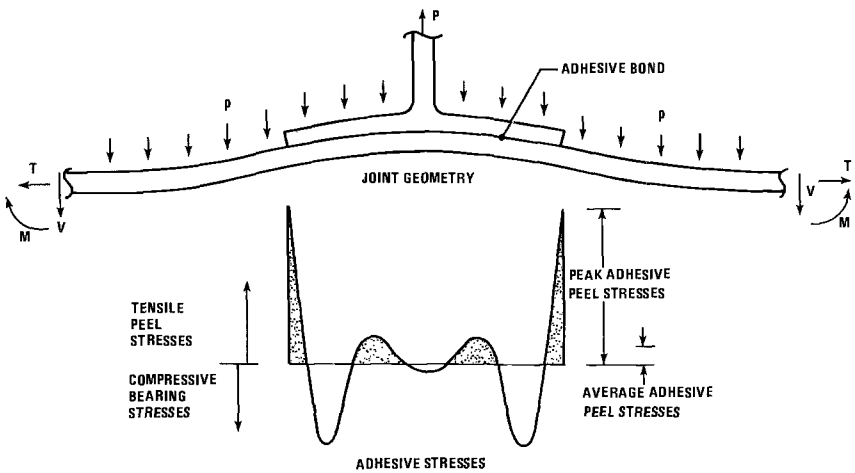

FIG. 22—*Peel stress distribution between stiffener and skin.*

in Fig. 23. These considerations include both manufacturing and engineering aspects of the design.

The effectiveness of these design details is well demonstrated by the failure of the stiffener rather than the adhesive in a shear panel test (Fig. 24). Examination of the adhesive fillet did not even reveal any crazing. Yet the stiffener web had been ripped off the flange in the area where the skin buckled. This provides a very convincing demonstration that adhesive peel stresses need not compromise the design of efficient structure.

Conclusions

Adhesive peel stresses that appear to be such a problem in test coupons can be reduced to a level of insignificance by proper proportioning of the details in structural joints. The joints assessed range from the double-lap joint with low induced peel stresses, through unsupported single-lap joints having moderate peel stresses, to flush single-strap joints that can develop intense peel stresses in the adhesive. In every case, it was shown that an adequate overlap and local tapering of the adherends to thin them at the ends of the overlaps were sufficient to alleviate all concern about peel stresses. Even the skin-to-stiffener bonds subjected to directly applied peel loads had been shown by extensive testing during the PABST program to not be a source of weakness.

The analyses discussed here indicate that it is important to recognize that there are tremendous differences between the behavior of adhesive bonds in

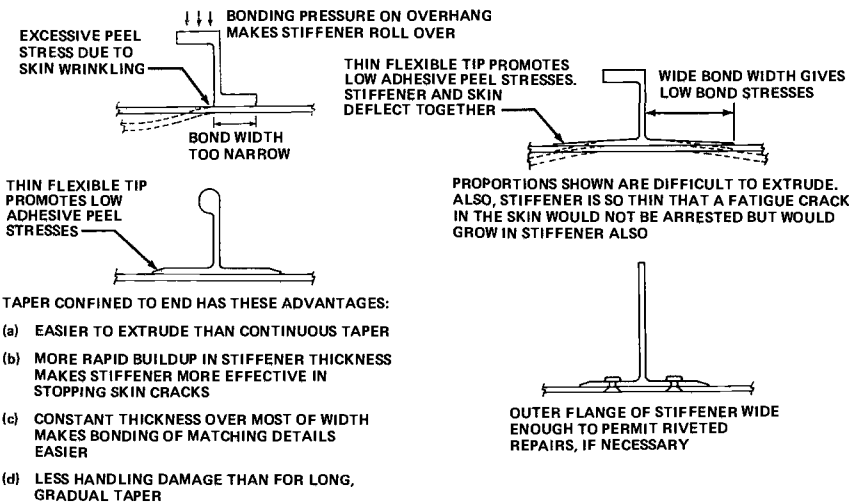

FIG. 23—*Considerations in the proportioning of bonded stiffeners.*

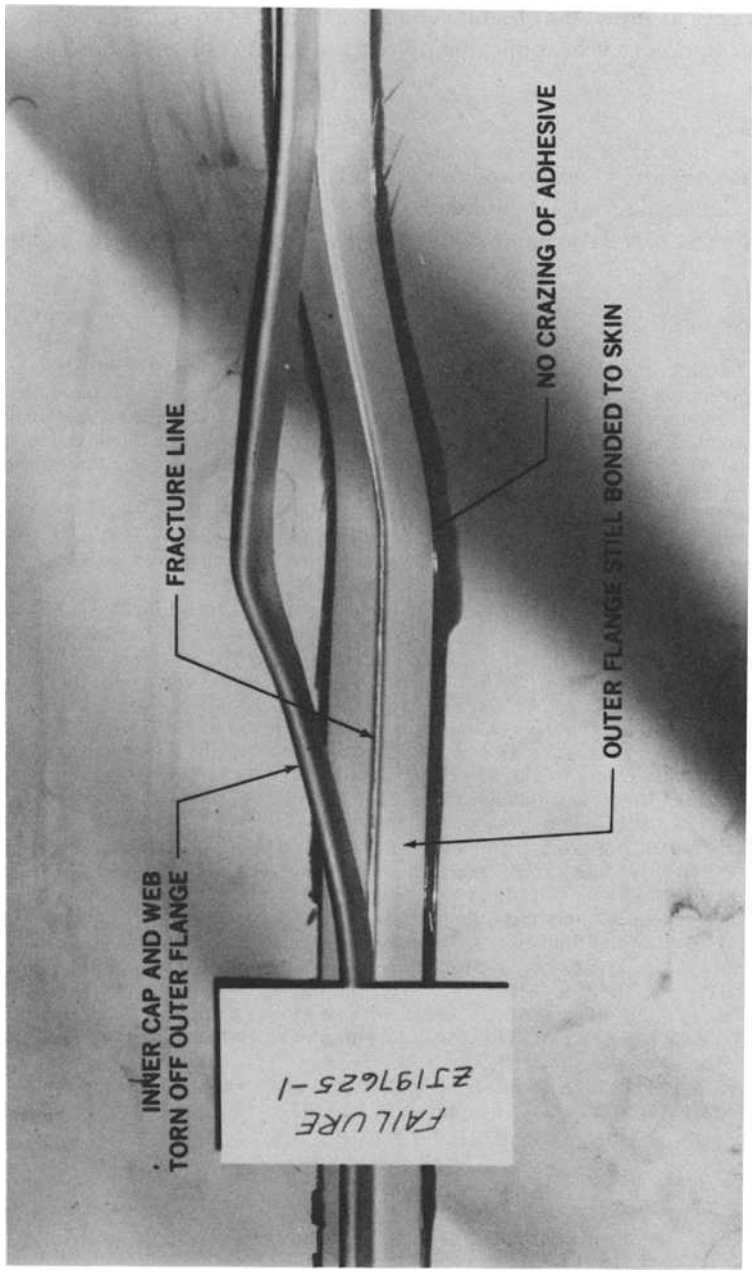

FIG. 24—*Shear panel failure showing tearing apart of bonded longeron.*

test coupons and in structurally configured joints. This is particularly true for peel stresses. Because of the different combinations of adhesive peel and shear stresses as functions of joint geometry, testing of coupons often reveals little information that is applicable to joints of other configurations.

Acknowledgment

The work reported here was performed at Douglas Aircraft Company, Long Beach, California, mainly under USAF Contract F33615-80-C-5092. H. S. Schwartz of the Air Force Materials Laboratory was the project monitor.

References

[1] Hart-Smith, L. J., "Design and Analysis of Bonded Repairs for Metal Aircraft Structures" in *Proceedings*, International Workshop on Defense Applications of Advanced Repair Technology for Metal and Composite Structures, Naval Research Laboratory, Washington, DC, July 1981; also published as Paper DP 7089 by Douglas Aircraft Co., Long Beach, CA.

[2] Renton, W. J., "The Symmetric Lap-Shear Test—What Good is It?," *Experimental Mechanics*, Vol. 16, Nov. 1976, pp. 409-415.

[3] Krieger, R. B., Jr., "Fatigue Testing of Structural Adhesives" in *The Enigma of the Eighties: Environment, Economics, Energy*, SAMPE Engineering Series, Vol. 24, Book 2; *Proceedings*, 24th National SAMPE Symposium and Exhibition, Society of Aerospace Material and Process Engineers, San Francisco, CA, May 1979, pp. 1102-1125.

[4] Hart-Smith, L. J., "Adhesive Layer Thickness and Porosity Criteria for Bonded Joints," USAF Report AFWAL-TR-82-4172, Air Force Wright Aeronautical Laboratories, Dec. 1982.

[5] Goland, M. and Reissner, E., "The Stresses in Cemented Joints," *Journal of Applied Mechanics*, Vol. 11, 1944, pp. A17-A27.

[6] Hart-Smith, L. J., "Differences Between Adhesive Behavior in Test Coupons and Structural Joints," presented to the ASTM Committee D-14 meeting, Phoenix, AZ, March 1981; published as Douglas Paper DP 7066 by Douglas Aircraft Co., Long Beach, CA.

[7] Hart-Smith, L. J., "Adhesive-Bonded Single-Lap Joints," NASA Langley Research Center, Report NASA CR 112236, Hampton, VA, Jan. 1973.

[8] Thrall, E. W., Jr., "Failures in Adhesively Bonded Structures," AGARD-NATO Lecture Series 102, Bonded Joints and Preparation for Bonding, Oslo, Norway, and The Hague, The Netherlands, April 1979, and Dayton, OH, Oct. 1979; also published as Douglas Paper DP 6703 by Douglas Aircraft Co., Long Beach, CA.

[9] Jones, W. B., Jr., and Romanko, J., "Fatigue Behavior of Adhesively Bonded Joints," in *Proceedings*, American Society of Mechanical Engineers, Winter Annual Meeting, Washington, DC, Nov. 1981, pp. 61-65.

[10] Clark, H. T., "Definition and Non-Destructive Detection of Critical Adhesive Bond-Line Flaws," USAF Report AFML-TR-78-108, Air Force Materials Laboratory, Wright-Patterson Air Force Base, Dayton, OH, July 1978.

[11] Hart-Smith, L. J., "Adhesive-Bonded Double-Lap Joints," NASA Langley Research Center, Report NASA CR 112235, Hampton, VA, Jan. 1973.